

Article 25fa pilot End User Agreement

This publication is distributed under the terms of Article 25fa of the Dutch Copyright Act (Auteurswet) with explicit consent by the author. Dutch law entitles the maker of a short scientific work funded either wholly or partially by Dutch public funds to make that work publicly available for no consideration following a reasonable period of time after the work was first published, provided that clear reference is made to the source of the first publication of the work.

This publication is distributed under The Association of Universities in the Netherlands (VSNU) 'Article 25fa implementation' pilot project. In this pilot research outputs of researchers employed by Dutch Universities that comply with the legal requirements of Article 25fa of the Dutch Copyright Act are distributed online and free of cost or other barriers in institutional repositories. Research outputs are distributed six months after their first online publication in the original published version and with proper attribution to the source of the original publication.

You are permitted to download and use the publication for personal purposes. All rights remain with the author(s) and/or copyrights owner(s) of this work. Any use of the publication other than authorised under this licence or copyright law is prohibited.

If you believe that digital publication of certain material infringes any of your rights or (privacy) interests, please let the Library know, stating your reasons. In case of a legitimate complaint, the Library will make the material inaccessible and/or remove it from the website. Please contact the Library through email: copyright@ubn.ru.nl, or send a letter to:

University Library
Radboud University
Copyright Information Point
PO Box 9100
6500 HA Nijmegen

You will be contacted as soon as possible.

Prostate Cancer: The European Society of Urogenital Radiology Prostate Imaging Reporting and Data System Criteria for Predicting Extraprostatic Extension by Using 3-T Multiparametric MR Imaging¹

Leonardo Kayat Bittencourt, MD, PhD
Geert Litjens, MSc
Christina A. Hulsbergen-van de Kaa, MD, PhD
Baris Turkbey, MD
Emerson Leandro Gasparetto, MD, PhD
Jelle O. Barentsz, MD, PhD

Purpose:

To retrospectively assess the use of the European Society of Urogenital Radiology (ESUR) Prostate Imaging Reporting and Data System (PI-RADS) criteria and 3-T multiparametric magnetic resonance (MR) imaging for detection of extraprostatic extension (EPE) of prostate cancer.

Materials and Methods:

The institutional review board approval requirement was waived. Consecutive patients with prostate cancer ($n = 133$) underwent 3-T multiparametric MR imaging before prostatectomy. Lesions were assessed by using ESUR/PI-RADS criteria for T2-weighted, diffusion-weighted, and dynamic contrast material-enhanced imaging, and by using the sum of these scores. Zonal dominant parameters corresponding to the score of diffusion-weighted imaging for peripheral zone lesions and to T2-weighted imaging scores for transitional zone lesions were calculated. In addition, the presence of EPE in each patient was evaluated on the basis of subjective multiparametric MR imaging features. Histopathologic examination of whole-mount radical prostatectomy specimens was used as the reference standard. Sensitivity, specificity, positive predictive, and negative predictive values; likelihood ratios; and areas under the receiver operating characteristic curve were calculated for each parameter on the basis of its usefulness for prediction of EPE.

Results:

EPE was found in 60 of 133 (45%) patients. Receiver operating characteristic curve analysis for the prediction of EPE revealed an area under the curve of 0.72 for T2-weighted, 0.67 for diffusion-weighted, and 0.64 for dynamic contrast-enhanced imaging; 0.74 for the dominant parameter; and 0.74 for the sum of the PI-RADS scores, and a score of 5 was defined as the best threshold for the individual parameters, with a score greater than or equal to 13 as the threshold for the sum of the PI-RADS scores. By applying these thresholds, sensitivity, negative predictive value, and negative likelihood ratio (ruling out EPE) were 77%, 77%, and 0.36, respectively, and specificity, positive predictive value, and positive likelihood ratio (ruling in EPE) were 64%, 64%, and 2.15, respectively, for the dominant parameter. Feature analysis showed an area under the curve of 0.72; sensitivity, negative predictive value, and negative likelihood ratio of 63%, 72%, and 0.56, respectively, and specificity, positive predictive value, and positive likelihood ratio of 78%, 70%, and 3.77, respectively.

Conclusion:

ESUR/PI-RADS criteria showed moderate overall accuracy for use in the prediction of EPE, and these results were similar to those of multiparametric MR imaging assessment of features in this study sample.

© RSNA, 2015

Online supplemental material is available for this article.

¹From the Department of Radiology, Radboud University Nijmegen Medical Centre, Nijmegen, the Netherlands (L.K.B., G.L., C.A.H.v.d.K., J.O.B.); Department of Radiology, Av Brigadeiro Trompowsky 255, Ilha do Fundão, Rio de Janeiro, RJ, Brazil 21941-913 (L.K.B., E.L.G.); Department of Radiology, Clínica de Diagnóstico por Imagem (CDPI), Rio de Janeiro, Brazil (L.K.B., E.L.G.); and Molecular Imaging Program, National Cancer Institute, National Institutes of Health, Bethesda, Md (B.T.). Received June 16, 2014; revision requested August 14; revision received October 27; accepted November 24; final version accepted January 15, 2015. Address correspondence to L.K.B. (e-mail: lkayat@gmail.com).

Multiparametric magnetic resonance (MR) imaging has emerged as one of the most promising techniques for the detection and characterization of prostate cancer (1,2). Staging of prostate cancer is one of the most appealing indications for multiparametric MR imaging, because the choice of treatment is directly

affected by the distinction between organ-confined disease (stages T1 and T2) and extraprostatic extension (EPE; stages T3 and T4). Patients with EPE are at greater risk for lymph node or bone metastases and for tumor recurrence after prostatectomy or radiotherapy (3,4), and they often need adjuvant therapy (5). Moreover, those patients cannot be subjected to bilateral nerve-sparing surgical techniques, which increase the risk for urinary incontinence and erectile dysfunction after prostatectomy (6).

Although conventional methods of staging based on digital rectal examination, prostate-specific antigen level, and transrectal ultrasonographic findings result in substantial levels of clinical understaging (59%) and some overstaging (5%) (7), adding multiparametric MR imaging to clinical data has been shown to result in increased accuracy for prediction of tumor stage and the presence of EPE. Authors of a previous study (8) on the prediction of EPE based on T2-weighted imaging described findings that included asymmetry of the neurovascular bundle, tumor encasement of the neurovascular bundle, a bulging prostatic contour, an irregular or spiculated margin, obliteration of the rectal-prostatic angle, capsular retraction, a tumor-capsule interface of greater than 1 cm, and a breach of the capsule with evidence of direct tumor extension. Other authors (9) who used T2-weighted and 3-T MR imaging reported maximum sensitivity and specificity of 80%–88% and 96%–100%, respectively, for the detection of EPE. However, the results of different multiparametric MR imaging prostate cancer staging studies (8,10,11) seem conflicting and generally show a wide

range of sensitivity (23%–90%) and specificity (30%–95%) values. This may be explained by the differences in field strengths, sequence and coil types, addition of multiparametric information, end-point definitions, patient selection, and also by the subjectivity and heterogeneity in the application of imaging criteria by the readers.

The development of the 2012 European Society of Urogenital Radiology (ESUR) prostate MR guidelines (12) is one of the most recent and comprehensive initiatives toward the standardization of prostate multiparametric MR imaging reporting and communication and included introduction of the Prostate Imaging Reporting and Data System (PI-RADS). Findings of multiparametric MR imaging of the prostate are scored on a 1–5 scale for each of the parameters of evaluation, with a score of 1 indicating that clinically significant disease is highly unlikely to be present; 2, unlikely to be present; 3, presence of disease equivocal; 4, likely to be present; and 5, highly likely to be present (Table E1, Fig E1 [online]).

Previously, authors of a few studies (13–16) assessed the ESUR/PI-RADS scoring system, focusing on the ability to detect prostate cancer lesions or the validation of ESUR/PI-RADS criteria. However, considering that local

Advances in Knowledge

- The European Society of Urogenital Radiology (ESUR) and Prostate Imaging Reporting and Data System (PI-RADS) scoring for multiparametric prostate MR imaging may help in the prediction of the presence of extraprostatic extension (EPE) in patients with prostate cancer.
- The dominant parameter exhibited the best accuracy overall among the assessment categories, with a sensitivity of 77% (46 of 60), a specificity of 64% (47 of 73) and an area under the curve of 0.74 for the detection of EPE in the whole patient sample.
- Diffusion-weighted imaging was the individual parameter with the highest accuracy (area under the curve, 0.70) for prediction of EPE in the peripheral zone, whereas T2-weighted imaging showed the highest accuracy in the transitional zone (area under the curve, 0.79), which supports the concept of a dominant parameter related to the zonal anatomy of prostate cancer lesions.
- A score greater than or equal to 4 for T2-weighted imaging was required to rule out the presence of EPE, with a sensitivity of 98% (59 of 60), negative predictive value of 96% (23 of 24), and negative likelihood ratio of 0.05 for the T2-weighted parameter; however, this benefit comes at the expense of lower specificity (32% [23 of 73]) and positive predictive value (54% [59 of 109]).

Implication for Patient Care

- The standardized ESUR/PI-RADS criteria can be applied for the detection of extraprostatic extension of prostate cancer with moderate overall accuracy, but larger prospective studies involving different cohorts are needed for further validation.

Published online before print

10.1148/radiol.15141412 Content code: **GU**

Radiology 2015; 276:479–489

Abbreviations:

AUC = area under the curve

CI = confidence interval

EPE = extraprostatic extension

ESUR = European Society of Urogenital Radiology

PI-RADS = Prostate Imaging Reporting and Data System

Author contributions:

Guarantors of integrity of entire study, L.K.B., E.L.G., J.O.B.; study concepts/study design or data acquisition or data analysis/interpretation, all authors; manuscript drafting or manuscript revision for important intellectual content, all authors; approval of final version of submitted manuscript, all authors; agrees to ensure any questions related to the work are appropriately resolved, all authors; literature research, L.K.B., B.T., E.L.G.; clinical studies, C.A.H.v.d.K., J.O.B.; experimental studies, L.K.B., G.L.; statistical analysis, L.K.B., G.L.; and manuscript editing, all authors

Conflicts of interest are listed at the end of this article.

Table 1

Detection and Staging MR Imaging Protocols

Protocol	Detection Sequences			Staging Sequences		
	T2 Weighted	Diffusion Weighted	Dynamic Contrast Enhanced	T2 Weighted	Diffusion Weighted	Dynamic Contrast Enhanced
Repetition time (msec)/echo time (msec)	4000/101	3300/60	3.8/1.42	4970/96	4000/76	36/1.4
Field of view (mm)	200 × 200	260 × 211	260 × 260	180 × 180	192 × 256	192 × 192
Matrix	320 × 320	160 × 130	160 × 160	320 × 320	96 × 128	128 × 128
Section thickness (mm)	3	3.6	3.6	3	3	3
Gap (%)	10	10	...	0	10	...
No. of averages	3	8	1	2	8	1
In-plane resolution (mm)	0.625 × 0.625	1.625 × 1.623	1.625 × 1.625	0.56 × 0.56	2.0 × 2.0	1.5 × 1.5
<i>b</i> value (sec/mm ²)	...	0, 100, 400, 800	50, 400, 800	...
No. of sections	20	20	20	20	20	20
Temporal resolution (sec)	2.5	3.5

staging of prostate cancer may play a key role in the definition of tumor aggressiveness, it remains to be determined whether the standardized ESUR/PI-RADS criteria can provide information for the prediction of EPE of prostate cancer. The purpose of our study was to retrospectively assess the use of the ESUR/PI-RADS criteria with 3-T multiparametric MR imaging to provide information for the detection of EPE of prostate cancer.

Materials and Methods

Patients

The requirement to obtain institutional review board approval was waived for this retrospective study. Inclusion criteria were prostate cancer treated by means of radical prostatectomy and preprostatectomy 3-T multiparametric MR imaging, including T2-weighted, diffusion-weighted, and dynamic contrast material-enhanced imaging, with prospective classification of each parameter evaluated according to ESUR/PI-RADS criteria. Exclusion criteria were previous radiation therapy and/or hormonal blockade or an interval longer than 6 months between MR imaging examination and prostatectomy.

Between January 2010 and May 2013, 181 consecutive patients underwent radical prostatectomy at our referral center,

and histopathologic specimens were submitted for whole-mount processing. Nine patients underwent prostatectomy more than 6 months after MR imaging examination, five patients had previously undergone radiation therapy, and 34 patients had no preoperative MR imaging reports containing ESUR/PI-RADS scores. Thus, 133 patients met the inclusion criteria for our study, with a mean interval of 2.6 months (range, 0.1–5.6 months) between MR imaging examination and prostatectomy.

MR Imaging Protocol

MR images were obtained by using one of two 3-T MR imaging systems (Trio Tim and Magnetom Skyra; Siemens, Erlangen, Germany). Detection protocols were used in 44 patients, and staging protocols were used in 89 patients according to the 2012 ESUR prostate MR guidelines (12). These protocols included high-spatial-resolution T2-weighted imaging in the axial, sagittal, and coronal planes, diffusion-weighted imaging in the axial plane (*b* values: 0–100, 400, and 800 sec/mm²), and dynamic contrast-enhanced imaging with the main MR imaging acquisition parameters described in Table 1.

The combination of a pelvic phased-array coil and an endorectal coil (Medrad, Pittsburg, Pa) filled with 40 mL of perfluorocarbon (Fomblin; Solvay-Solexis, Milan, Italy) was used in the

staging protocol, whereas the detection protocol was performed by using only a pelvic phased-array coil. Peristalsis was suppressed by means of an intramuscular injection of 1 mg of glucagon (Glucagen; Nordisk, Gentofte, Denmark).

Apparent diffusion coefficient maps were calculated by using mono-exponential fitting to the *b*-value data, excluding the images acquired with a *b* value of 0 sec/mm². Postprocessing of dynamic contrast-enhanced MR imaging data was performed by using software developed in-house (17). The in-house software generated semiquantitative curves (ie, relative enhancement vs time) derived from dynamic contrast-enhanced imaging data. For the scoring of the dynamic contrast-enhanced imaging component of ESUR/PI-RADS, these curves were overlaid and coregistered with the same locations as those in axial T2-weighted and diffusion-weighted imaging data, on a voxel-by-voxel basis.

MR Imaging Interpretation and ESUR/PI-RADS Classification

One radiologist (J.O.B., with 20 years of experience with prostate MR imaging and experience with PI-RADS) prospectively read and scored all cases by using software developed in-house (17) that generated a standardized structured report for each patient. The radiologist was informed of each patient's clinical

data, including the indication for the study, prostate-specific antigen levels, and biopsy results when available.

In the structured report, each region suspected to be cancer was graded according to the ESUR/PI-RADS criteria for T2-weighted (for either the peripheral or transitional zone), diffusion-weighted, and dynamic contrast-enhanced imaging parameters (Fig E1 [online]). A score ranging from 1 to 5 was given for each parameter, according to the probability of clinically significant prostate cancer (ie, Gleason Score ≥ 7 , tumor volume ≥ 0.5 mL, and/or signs of EPE) (12). In addition, the simple sum of the individual parameters also was calculated, with the resulting values ranging from 3 to 15. For patients with more than one region suspected to be cancer, only the region with the highest sum of the PI-RADS scores was used for statistical analysis. Regions suspected to be cancer also were marked according to a 27-region scheme previously described for the prostate gland (18), with their locations classified as predominantly in the peripheral or transitional zone.

According to the zonal location of the highest-rated region suspected to be cancer in each patient, a new individual parameter called the dominant parameter was created, with an aim to investigate the possible predominance of diffusion-weighted imaging findings in the peripheral zone and of T2-weighted findings in the transitional zone, as suggested by authors of recent studies (19,20). Therefore, the score of the dominant parameter was equal to the diffusion-weighted imaging score in patients with peripheral zone lesions and equal to the T2-weighted score in patients with transitional zone lesions.

As a part of every structured report and regardless of the ESUR/PI-RADS scoring, each patient also was rated (J.O.B.) for the likelihood of EPE on the basis of morphologic multiparametric MR imaging features that are generally accepted by researchers (8,9,21). The reports included three assessment categories: no signs of EPE, minimal or dubious EPE, or suspected EPE.

For statistical purposes, patients rated with minimal or dubious EPE and suspected EPE were grouped as positive for the presence of EPE, whereas those with no signs of EPE were considered negative.

Histopathologic Analysis

Radical prostatectomy specimens were sectioned into 4-mm axial step sections and were whole-mount processed. A urogenital pathologist (C.H.v.d.K., with more than 18 years of experience) prospectively determined the location, dimensions, stage, and Gleason grade components for each individual tumor according to the 2005 International Society of Urological Pathology criteria (22). In the prostatectomy reports, EPE was further classified as minimal or focal in the presence of extracapsular extension or as showing bladder-neck involvement with a maximal radial diameter of less than or equal to 0.6 mm, whereas extensive or established EPE was defined as a maximal radial diameter greater than 0.6 mm or any sign of seminal vesicle involvement (23). However, for the purpose of statistical analysis, EPE was defined in our study as the presence of any type or classification of extracapsular extension, seminal vesicle involvement, or bladder-neck invasion. Organ-confined disease was defined as the absence of these three conditions.

Statistical Analyses

Analyses were performed by using software (SPSS Statistics version 20; SPSS, Chicago, Ill, and MedCalc; MedCalc Software, Ostend, Belgium). A two-sided *P* value less than .05 was considered to indicate a significant difference. Each parameter was assessed for its accuracy when used for prediction of the presence or absence of EPE in the whole set of patients and in subgroups of peripheral and transitional zone tumors separately. Mean values \pm standard deviations were calculated for the scores for each group and were compared by using an independent *t* test for continuous variables.

Cutoff values for the ESUR/PI-RADS parameters were estimated from the

Table 2

Patient and Prostatectomy Characteristics

Parameter	Data
No. of patients	133
Clinical demographics	
Median prostate-specific antigen (ng/mL)*†	8.6 (2.5–76.0)
Mean age (y)*	61 (47–72)
Pathologic demographics	
Peripheral zone tumors‡	83 (62)§
Transitional zone tumors‡	50 (38)§
Organ-confined disease	73 (55)
EPE	60 (45)
Extensive EPE	46 (77)
Focal EPE	14 (23)
Gleason score	
5	9 (7)
6	33 (25)
7	73 (55)
8	6 (5)
9	10 (8)
10	2 (2)
EPE findings per Gleason score#	
5	2/9 (22)
6	3/33 (9)
7	43/73 (59)
8	4/6 (67)
9	6/10 (60)
10	2/2 (100)
Stage	
pT2a	11 (8)
pT2b	1 (0.8)
pT2c	61 (46)
pT3a	44 (33)
pT3b	11 (8)
pT4	5 (4)

Note.—Unless otherwise indicated, data are number of patients, with percentage in parentheses.

* Data in parentheses are the range.

† To convert to Système International units (micrograms per liter), multiply by 1.

‡ Dominant tumor focus.

§ Indicates a significant difference (*P* < .0001).

Data are proportions of patients with EPE of total patients with each score, with percentage in parentheses.

best operating points of receiver-operating characteristic curve analyses by using the Youden *J* statistic (sensitivity + specificity – 1), corresponding to a score of 5 for each individual parameter and a score greater than or equal to

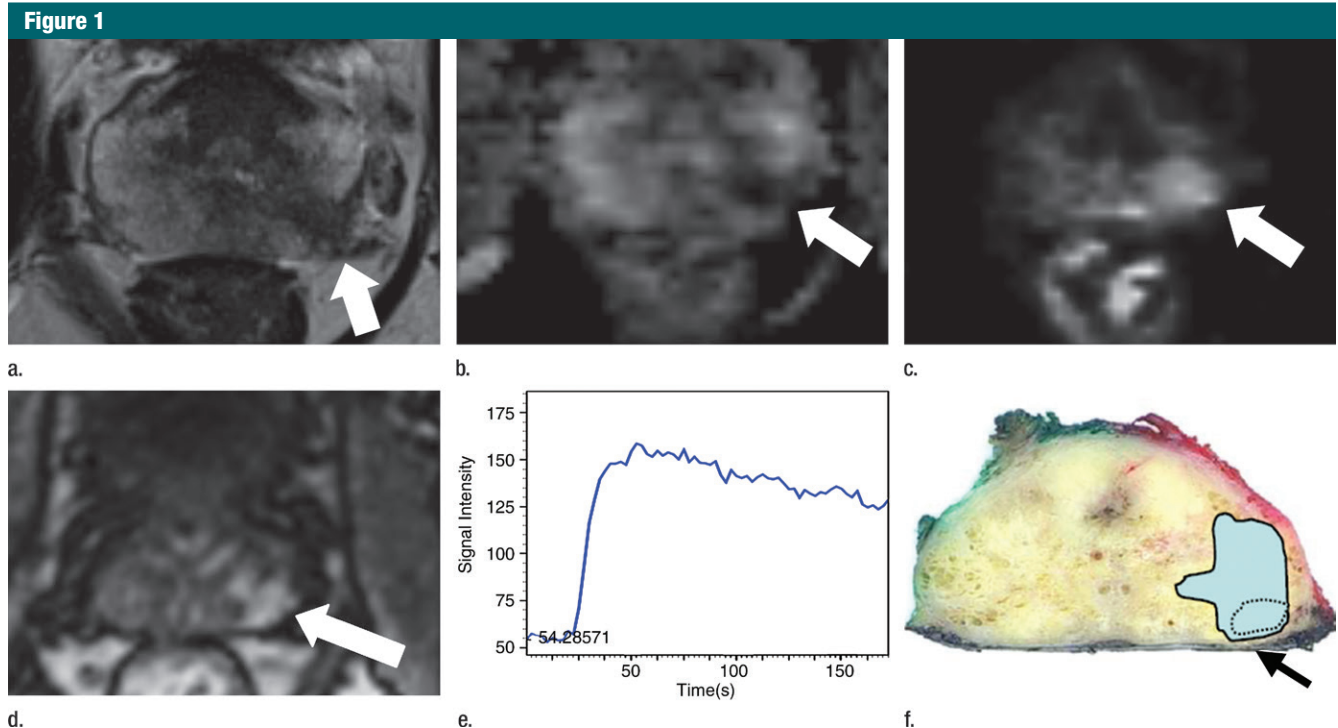


Figure 1: Typical multiparametric MR imaging findings suspicious for prostate cancer based on ESUR/PI-RADS criteria in 67-year-old patient. **(a)** T2-weighted axial image (repetition time msec/echo time msec, 4260/99) shows oval-shaped, irregular T2 hypointense focal lesion in posterolateral left mid gland peripheral zone (arrow) that promoted focal bulging of capsular contour; image given score of 5. **(b)** Diffusion-weighted axial image shows apparent diffusion coefficient values (2000/67, $b = 0, 50, 500, 800 \text{ sec/mm}^2$) were focally low in corresponding area (arrow; apparent diffusion coefficient, $0.75 \times 10^{-3} \text{ mm}^2/\text{sec}$). **(c)** Original diffusion-weighted image shows focal high signal intensity (arrow; $b = 800 \text{ sec/mm}^2$); image given score of 5. **(d)** Axial dynamic contrast-enhanced image from early arterial phase shows focal asymmetric area with early and intense contrast enhancement (arrow), and **(e)** signal intensity versus time curve shows type 3 curve with washout; image given score of 5. Consequently, the sum of PI-RADS scores was 15. Because lesion was in peripheral zone, diffusion-weighted imaging was deemed the dominant parameter; image given score of 5. At feature analysis, this study was rated as highly suspicious for EPE. **(f)** Whole-mount histopathologic section from prostatectomy specimen shows that lesion suspicious for cancer on multiparametric MR images corresponded to Gleason 7 (3+4) prostate cancer, and pathologist reported extracapsular extension at location indicated by arrow (dotted area represents Gleason 4 component hotspot).

13 for the sum of the PI-RADS scores. Those cutoff values were validated by means of k -fold cross-validation ($k = 4$), and the averages and standard deviations of the relevant statistics from the four folds were compared with the results of the whole sample.

In addition and according to the definitions provided in the ESUR prostate MR imaging guidelines (12), an arbitrary score of greater than or equal to 4 for each individual parameter was evaluated as an alternative threshold value for the prediction of EPE. Sensitivities, specificities, positive predictive values, negative predictive values, positive likelihood ratios, and negative likelihood ratios were calculated for these parameters to evaluate their ability to

allow prediction of EPE in the whole gland, the peripheral zone subgroup, and the transitional zone subgroup.

Results

Radical prostatectomy specimens revealed dominant prostate cancer lesions in the peripheral zone in 83 of 133 (62%) patients and in the transitional zone in 50 of 133 (38%) patients. EPE was found in 60 of 133 (45%) patients, whereas 73 of 133 (55%) had organ-confined disease. Patient characteristics are described in Table 2. In addition, an example of a patient with clinically significant cancer correlated to ESUR/PI-RADS criteria on the basis of MR imaging findings is shown in Figure 1.

Histograms and column charts were generated to help analyze the frequency of the individual and composite scores for this cohort, along with the prevalence of focal and established EPE (Fig E2 [online]). Most of the individual parameters received scores of 4 or 5, which also were reflected as a predominance of high values in the sum of the PI-RADS scores. This is most probably due to the composition of the study population, which consisted only of patients with confirmed prostate cancer.

Analysis by means of k -fold cross-validation ($k = 4$) showed no significant differences among the averaged results (sensitivity, specificity, negative predictive value, positive predictive value, and area under the curve [AUC])

throughout the fourfolds and the results obtained from the whole study sample. As such, for clarity, we present the results throughout the whole set of patients. The results of the cross-validation are presented in Table 3.

Mean values \pm standard deviation for the ESUR/PI-RADS parameter scores are summarized in Table 4. The results are categorized according to EPE versus prediction of organ-confined disease for the entire cohort, the peripheral zone subgroup, and the transitional zone subgroup. Differences between each group were statistically significant for each parameter evaluated, except for those between diffusion-weighted imaging ($P = .13$) and dynamic contrast-enhanced imaging ($P = .38$) of transitional zone lesions. However, despite the statistical significance, there was still a considerable overlap of means and standard deviations between the scores of patients with and those without EPE for all of the parameters.

The individual parameters (ie, T2-weighted, diffusion-weighted, and dynamic contrast-enhanced imaging, and the dominant parameter) and the sum of the PI-RADS scores showed moderate to good sensitivity (55%–80%) and specificity (51%–73%) for the prediction of EPE (Table 5). Among all of the ESUR/PI-RADS variables that were investigated, the dominant parameter showed the best combination of results, with a score of 5 granting a sensitivity of 77% (46 of 60; 95% CI: 64, 86), a specificity of 64% (47 of 73; 95% CI: 52, 75), a positive predictive value of 64% (46 of 72; 95% CI: 51, 74), a negative predictive value of 77% (47 of 61; 95% CI: 64, 87), a positive likelihood ratio of 2.15 (95% CI: 1.5, 3.0), and a negative likelihood ratio of 0.36 (95% CI: 0.2, 0.6). The sum of the PI-RADS scores showed accuracy that was similar to that of the dominant parameter for the entire cohort, with a cutoff value greater than or equal to 13 granting sensitivity of 73% (44 of 60; 95% CI: 60, 84), specificity of 64% (47 of 73; 95% CI: 52, 75), a positive predictive value of 63% (44 of 70; 95% CI: 50, 74), a negative predictive value of 75% (47 of 63; 95% CI: 62, 84), a

Table 3
Whole Sample and Fourfold Cross-Validation Results

Parameter	Whole Sample					Fourfold Cross Validation Testing Sets				
	T2 Weighted	Diffusion Weighted	Dynamic Contrast Enhanced	Dominant	Sum of PI-RADS	T2 weighted	Diffusion weighted	Dynamic Contrast Enhanced	Dominant	Sum of PI-RADS
Criteria	5	5	5	5	≥ 13	4.75 \pm 0.5	5	5	5	$\geq 12.5 \pm 0.6$
Sensitivity (%)	68	80	55	77	73	72.16 \pm 18.7	81.65 \pm 8.9	55.65 \pm 11.0	78.23 \pm 11.9	79.30 \pm 12.7
Specificity (%)	68	55	73	64	64	52.69 \pm 17.6	52.44 \pm 12.0	74.30 \pm 15.4	64.60 \pm 7.4	53.45 \pm 13.1
Positive predictive value (%)	64	57	62	64	63	56.25 \pm 10.2	58.43 \pm 13.9	64.48 \pm 22.7	64.13 \pm 11.7	58.15 \pm 15.2
Negative predictive value (%)	72	76	66	77	75	73.10 \pm 22.3	76.88 \pm 14.1	52.90 \pm 33.5	77.08 \pm 17.6	76.08 \pm 14.7
Positive likelihood ratio	2.17	1.62	2.01	2.15	2.06	1.62 \pm 0.40	1.76 \pm 0.27	3.17 \pm 2.58	2.32 \pm 0.82	1.78 \pm 0.44
Negative likelihood ratio	0.46	0.39	0.62	0.36	0.41	0.48 \pm 0.33	0.34 \pm 0.11	0.63 \pm 0.23	0.35 \pm 0.20	0.39 \pm 0.20
AUC	0.72	0.67	0.64	0.74	0.74	0.72 \pm 0.13	0.69 \pm 0.05	0.65 \pm 0.12	0.74 \pm 0.06	0.75 \pm 0.11

Note.—Unless otherwise indicated, data are means \pm standard deviation.

Table 4

Individual Parameter and Sum of PI-RADS Scores for Presence of EPE

Parameter	EPE Whole Gland		Organ-confined Disease		P Value	EPE Peripheral Zone		Organ-confined Disease		P Value	EPE Transitional Zone		Organ-confined Disease		P Value
	Mean ± SD	95% CI	Mean ± SD	95% CI		Mean ± SD	95% CI	Mean ± SD	95% CI		Mean ± SD	95% CI	Mean ± SD	95% CI	
T2 weighted	4.65 ± 0.58	4.12 ± 1.03	3.93 ± 0.92	3.74 ± 1.12	<.0001	4.64 ± 0.63	4.07 ± 0.92	4.07 ± 0.92	4.07 ± 0.92	.0013	4.67 ± 0.48	3.72 ± 0.88	3.72 ± 0.88	<.0001	
Diffusion weighted	4.73 ± 0.61	4.12 ± 1.03	4.12 ± 1.03	3.74 ± 1.12	<.0001	4.77 ± 0.54	4.00 ± 1.10	4.00 ± 1.10	4.00 ± 1.10	.0001	4.67 ± 0.73	4.31 ± 0.89	4.31 ± 0.89	.1274	
Dynamic contrast enhanced	4.23 ± 1.09	3.74 ± 1.12	3.74 ± 1.12	3.74 ± 1.12	.0115	4.44 ± 0.94	3.86 ± 1.13	3.86 ± 1.13	3.86 ± 1.13	.0139	3.86 ± 1.27	3.55 ± 1.08	3.55 ± 1.08	.3802	
Dominant	4.73 ± 0.51	3.89 ± 1.02	3.89 ± 1.02	3.89 ± 1.02	<.0001	
Sum of PI-RADS	13.62 ± 1.64	11.79 ± 2.16	11.79 ± 2.16	11.79 ± 2.16	<.0001	13.85 ± 1.46	11.93 ± 2.24	11.93 ± 2.24	11.93 ± 2.24	<.0001	13.19 ± 1.88	11.59 ± 2.06	11.59 ± 2.06	.0065	

Note.—Unless otherwise indicated, data are means ± standard deviation.

positive likelihood ratio of 2.06 (95% CI: 1.5, 2.9), and a negative likelihood ratio of 0.41 (95% CI: 0.3, 0.7) for the prediction of EPE. Receiver operating characteristic curve analysis data were also consistent with these findings (Fig 2), with the curves of the dominant parameter and the sum of the PI-RADS scores exhibiting the highest discriminatory performance among all of the variables evaluated (AUC, 0.74; 95% CI: 0.66, 0.81).

For the peripheral zone subgroup, the sum of the PI-RADS scores (AUC, 0.75; 95% CI: 0.64, 0.84) and diffusion-weighted imaging (AUC, 0.70; 95% CI: 0.59, 0.79) showed generally better performance among the study variables. For the transitional zone subgroup, T2-weighted imaging showed the highest AUC for the prediction of EPE (AUC, 0.79; 95% CI: 0.66, 0.90).

The diagnostic performance of each parameter determined by applying an arbitrary score greater than or equal to 4 is summarized in Table 6. While the sensitivity associated with these parameters was considerably higher (82%–98%), the specificity decreased (27%–36%). Nevertheless, the negative predictive values were higher and negative likelihood ratios were substantially lower with the use of these thresholds, especially for T2-weighted imaging (negative predictive value, 96% [23 of 24]; 95% CI: 92, 99; negative likelihood ratio, 0.05; 95% CI: 0.0, 0.4) and the dominant parameter (negative predictive value, 93% [26 of 28]; 95% CI: 76, 99; negative likelihood ratio, 0.09; 95% CI: 0.02, 0.40).

Assessment based on morphologic multiparametric MR imaging features for the prediction of EPE (Table 5) revealed sensitivity of 63% (38 of 60, 95% CI: 55, 71), specificity of 78% (57 of 73, 95% CI: 71, 85), a positive predictive value of 70% (38 of 54, 95% CI: 62, 78), a negative predictive value of 72% (57 of 79, 95% CI: 64, 79), a positive likelihood ratio of 3.77 (95% CI: 2.0, 7.1), and a negative likelihood ratio of 0.56 (95% CI: 0.4, 0.7) for the whole gland, incorporating an AUC of 0.72 (95% CI: 0.63, 0.79). For the

peripheral zone and transitional zone subgroups, respectively, feature assessment showed similar AUCs to those of T2-weighted imaging, with ESUR/PI-RADS scores equal to 0.68 (95% CI: 57, 78) and 0.77 (95% CI: 63, 88).

Discussion

In our study, we investigated the use of the ESUR/PI-RADS criteria for the prediction of EPE in patients with prostate cancer. The dominant parameter exhibited the best accuracy among the ESUR/PI-RADS variables for the prediction of EPE in the whole gland, with an AUC of 0.74 (95% CI: 0.66, 0.81). In comparison, multiparametric MR imaging feature assessment based on commonly described morphologic criteria showed comparable results, with an AUC of 0.72 (95% CI: 0.63, 0.79) for prediction of EPE.

On the basis of receiver operating characteristic curve analysis, the dominant parameter was comparable to feature assessment in the whole gland (dominant parameter AUC vs feature AUC, 0.74 vs 0.72), with considerable overlap in the 95% CIs (0.65, 0.81 vs 0.63, 0.79, respectively). This similar performance could be partly explained by the fact that the ESUR/PI-RADS criteria for a T2-weighted score of 5 for peripheral zone and transitional zone lesions contained some of the descriptive features that were also used for feature assessment of EPE (Table E1 [online]). However, although AUCs can be similar, the analysis of receiver-operating characteristic curve shapes indicated slight differences in the sensitivity and specificity profiles of each rationale.

Feature assessment showed sensitivity of 63% (38 of 60) and specificity of 78% (57 of 73), in keeping with a high-specificity reading profile, an approach that radiologists traditionally chose to prevent incorrectly ruling out a patient for curative surgery (24), while trying to maintain a low false-positive ratio for EPE. In comparison, the ESUR/PI-RADS parameters exhibited a high-sensitivity profile, with the dominant parameter showing sensitivity of

Table 5
Accuracy for Detection of EPE in the Whole Gland and in Subgroups

Parameter	Sensitivity	Specificity	Positive Predictive Values	Negative Predictive Value	Positive Likelihood Ratio*	Negative Likelihood Ratio*	AUC*
EPE whole gland							
T2-weighted imaging score = 5	68 (41/60) [60, 76]	68 (50/73) [61, 76]	64 (41/64) [56, 72]	72 (50/69) [65, 80]	2.17 [1.5, 3.2]	0.46 [0.3, 0.7]	0.72 [0.64, 0.79]
Diffusion-weighted imaging score = 5	80 (48/60) [67, 89]	51 (37/73) [38, 62]	57 (48/84) [46, 68]	76 (37/49) [61, 87]	1.62 [1.2, 2.1]	0.39 [0.2, 0.7]	0.67 [0.58, 0.74]
Dynamic contrast-enhanced imaging score = 5	55 (33/60) [41, 68]	73 (53/73) [70, 82]	62 (33/53) [48, 75]	66 (53/80) [54, 76]	2.01 [1.3, 3.1]	0.62 [0.5, 0.8]	0.64 [0.72, 0.55]
Dominant score = 5							
Dominant score = 5	77 (46/60) [64, 86]	64 (47/73) [52, 75]	64 (46/72) [51, 74]	77 (47/61) [64, 87]	2.15 [1.5, 3.0]	0.36 [0.2, 0.6]	0.74 [0.65, 0.81]
Sum of PI-RADS scores = 13							
Sum of PI-RADS scores = 13	73 (44/60) [60, 84]	64 (47/73) [52, 75]	63 (44/70) [50, 74]	75 (47/63) [62, 84]	2.06 [1.5, 2.9]	0.41 [0.3, 0.7]	0.74 [0.66, 0.81]
Feature	63 (38/60) [55, 71]	78 (57/73) [71, 85]	70 (38/54) [62, 78]	72 (57/79) [64, 79]	3.77 [2.0, 7.1]	0.56 [0.4, 0.7]	0.72 [0.63, 0.79]
EPE peripheral zone							
T2-weighted imaging score = 5	69 (27/39) [52, 83]	61 (27/44) [45, 75]	61 (27/44) [45, 75]	69 (27/39) [52, 83]	1.79 [1.2, 2.7]	0.50 [0.3, 0.8]	0.68 [0.56, 0.78]
Diffusion-weighted imaging score = 5	82 (32/39) [66, 92]	55 (24/44) [38, 69]	62 (32/52) [47, 74]	77 (24/31) [58, 90]	1.81 [1.3, 2.6]	0.33 [0.2, 0.7]	0.70 [0.59, 0.79]
Dynamic contrast-enhanced imaging score = 5	64 (25/39) [47, 79]	68 (30/44) [52, 81]	64 (25/39) [47, 79]	68 (30/44) [52, 81]	2.01 [1.2, 3.3]	0.53 [0.3, 0.8]	0.66 [0.55, 0.76]
Sum of PI-RADS ≥ 13							
Sum of PI-RADS ≥ 13	74 (29/39) [58, 87]	61 (27/44) [45, 75]	63 (29/46) [47, 77]	73 (27/37) [56, 86]	1.92 [1.3, 2.9]	0.42 [0.2, 0.7]	0.75 [0.64, 0.84]
Feature	62 (24/39) [51, 72]	70 (31/44) [60, 80]	65 (24/37) [54, 75]	67 (31/46) [57, 77]	2.1 [1.2, 3.5]	0.55 [0.4, 0.8]	0.68 [0.57, 0.78]
EPE transitional zone							
T2-weighted imaging score = 5	67 (14/21) [43, 85]	79 (23/29) [60, 92]	70 (14/20) [46, 88]	77 (23/30) [58, 90]	3.22 [7.0, 1.5]	0.42 [0.2, 0.8]	0.79 [0.66, 0.90]
Diffusion-weighted imaging score = 5	76 (16/21) [53, 92]	45 (13/29) [26, 64]	50 (16/32) [32, 68]	72 (13/18) [46, 90]	1.38 [0.9, 2.1]	0.53 [0.2, 1.3]	0.61 [0.47, 0.74]
Dynamic contrast-enhanced imaging score = 5	38 (8/21) [18, 62]	79 (23/29) [60, 92]	57 (8/14) [29, 82]	64 (23/36) [46, 79]	1.84 [0.8, 4.5]	0.78 [0.5, 1.1]	0.60 [0.45, 0.73]
Sum of PI-RADS ≥ 13							
Sum of PI-RADS ≥ 13	71 (15/21) [48, 89]	69 (20/29) [49, 85]	62 (15/24) [41, 81]	77 (20/26) [56, 91]	2.30 [1.3, 4.2]	0.41 [0.2, 0.9]	0.72 [0.56, 0.84]
Feature	67 (14/21) [53, 79]	90 (26/29) [81, 98]	82 (14/17) [71, 93]	79 (26/33) [67, 90]	6.44 [2.1, 19.6]	0.37 [0.2, 0.7]	0.77 [0.63, 88]

Note.—Unless otherwise indicated, data are percentages, with numerators and denominators in parentheses and 95% confidence intervals (CIs) in brackets.

* Data in brackets are 95% CIs.

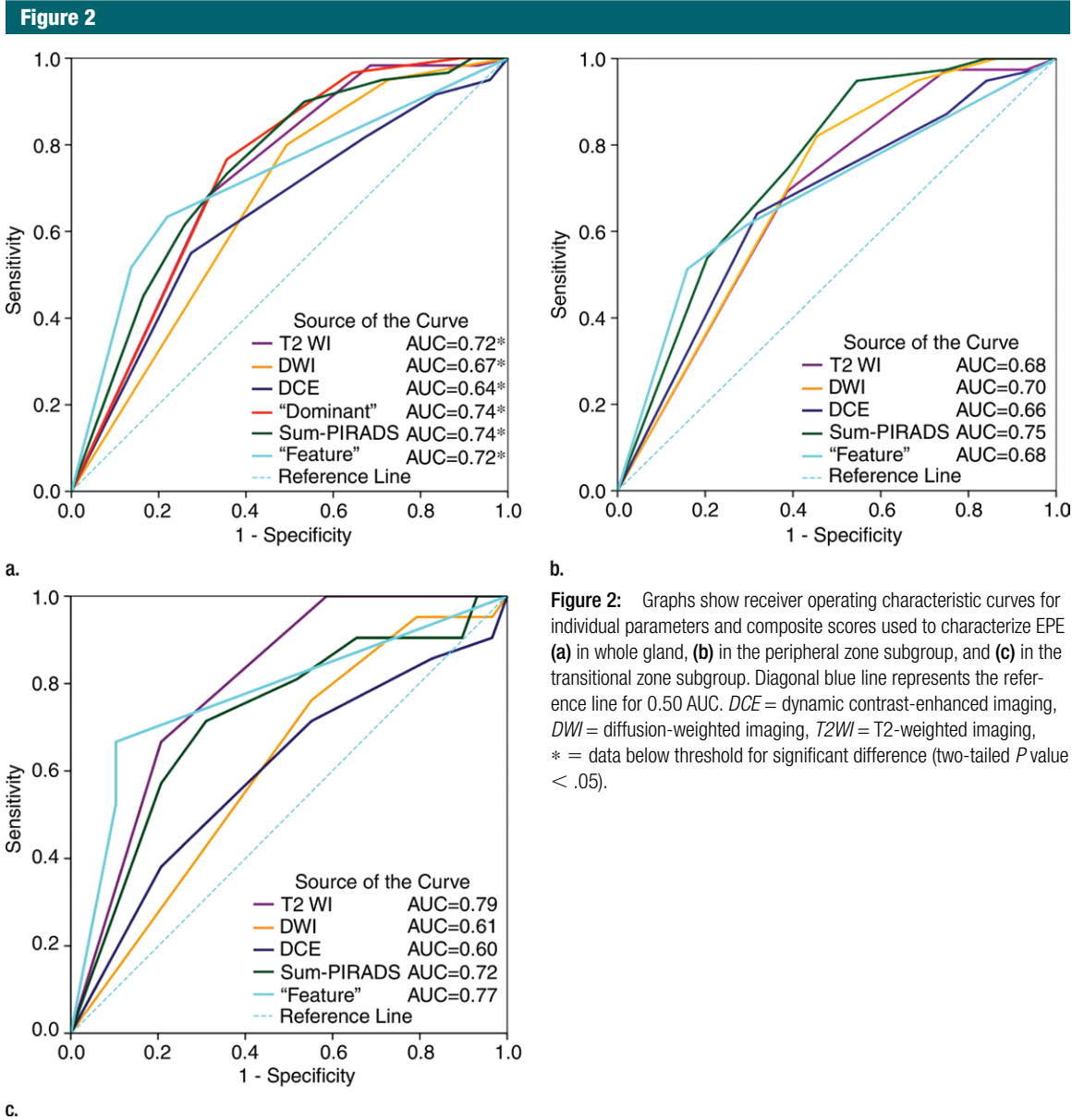


Figure 2: Graphs show receiver operating characteristic curves for individual parameters and composite scores used to characterize EPE (a) in whole gland, (b) in the peripheral zone subgroup, and (c) in the transitional zone subgroup. Diagonal blue line represents the reference line for 0.50 AUC. DCE = dynamic contrast-enhanced imaging, DWI = diffusion-weighted imaging, T2WI = T2-weighted imaging, * = data below threshold for significant difference (two-tailed *P* value < .05).

77% (46 of 60) and specificity of 64% (47 of 73) for the detection of EPE.

From a practical standpoint, we also observed that the adoption of an arbitrary threshold of greater than or equal to 4 for the scores of T2-weighted imaging and the dominant parameter was associated with a higher sensitivity profile for the detection of EPE. This is in line with the concept of high-sensitivity reading and may indicate a potential to rule out the presence of EPE effectively by adopting this approach. However, this

benefit comes at the cost of correspondingly lower specificity, such that a higher rate of false-positive results is expected. Nevertheless, despite false positivity for the presence of EPE, an ESUR/PI-RADS score of greater than or equal to 4 could still represent clinically significant prostate cancer, such as an organ-confined lesion with a high Gleason score.

In our study we also have introduced the concept of a zonal dominant parameter in an attempt to incorporate to ESUR/PI-RADS criteria the

performance of different techniques applied to peripheral and transitional zone lesions. In the assessment of the ESUR/PI-RADS criteria for the prediction of EPE based on the zonal anatomy of prostate cancer, diffusion-weighted imaging had the highest AUC among individual parameters in the subgroup of patients with peripheral zone lesions, while T2-weighted imaging showed the highest AUC in the subgroup of patients with transitional zone lesions. This result provides some support to our

Table 6

Accuracy for Detection of EPE in the Whole Gland with a Score of 4 or Higher

Parameter with Score of 4 or Higher	Sensitivity	Specificity	Positive Predictive Value	Negative Predictive Value	Positive Likelihood Ratio*	Negative Likelihood Ratio*
T2 weighted	98 (59/60) [96, 100]	32 (23/73) [24, 39]	54 (59/109) [46, 63]	96 (23/24) [92, 99]	1.44 [1.2, 1.7]	0.05 [0.00, 0.40]
Diffusion weighted	95 (57/60) [86, 99]	27 (20/73) [18, 39]	52 (57/110) [42, 61]	87 (20/23) [66, 97]	1.31 [1.1, 1.5]	0.18 [0.06, 0.60]
Dynamic contrast enhanced	82 (49/60) [68, 90]	33 (24/73) [22, 44]	50 (49/98) [39, 60]	69 (24/35) [50, 83]	1.22 [1.0, 1.5]	0.56 [0.3, 1.0]
Dominant	97 (58/60) [88, 99]	36 (26/73) [24, 47]	55 (58/105) [45, 65]	93 (26/28) [76, 99]	1.50 [1.3, 1.8]	0.09 [0.02, 0.40]

Note.—Unless otherwise indicated, data are percentages, with proportions of patients in parentheses and 95% CIs in brackets.

* Data in brackets are 95% CIs.

definition of the dominant parameter. However, despite the promising results demonstrated here, there was still considerable overlap in the 95% CIs, and this concept remains to be validated in larger prospective studies. It will be important to determine whether this type of parameter can be used on its own or for the development of new composite scores with different weightings among the original individual parameters.

Our study had a number of limitations. First, to optimize the reference standard used, we selected only patients who underwent prostatectomy, which may have introduced a verification bias into our results. As a consequence and considering that the test performance in clinical practice is strongly dependent on the prevalence of EPE and on the preoperative D'Amico risk category, the results of our study should be mostly applicable to a population with intermediate- to high-risk disease (Gleason scores > 6) and large-volume tumors (> pT2b) and cannot be extrapolated directly to a general screening population. Second, despite the potential differences between staging and detection protocols, preliminary subgroup analyses (not described in this article) did not provide statistically significant results to enable comparison between the protocols because of the small sample size in both subgroups. Therefore, additional studies may be needed to determine if the use of an endorectal coil influences ESUR/PI-RADS scoring. Third, because only a single reader prospectively interpreted the

images at the time of the examination, interobserver agreement was not assessed, and measurement bias could have been introduced, which makes it more difficult to generalize from our results. Fourth, because the primary intent of our study was to investigate the prediction of EPE on a per-patient basis, there was no direct comparison between each region suspected to be cancer at multiparametric MR imaging and each tumor focus detected at whole-mount histopathologic examination. It is possible that a per-lesion approach would have produced different results. Although a per-patient approach has been shown to be acceptable for evaluating EPE and staging information, which was the case in our study, this may not be true for studies in which Gleason score is used to evaluate prostate cancer aggressiveness, where a per-lesion approach would be preferred.

In conclusion, ESUR/PI-RADS criteria show moderate overall performance for the prediction of EPE, with similar results to those of morphologic feature-based multiparametric MR imaging assessment in our study sample, although with generally higher sensitivity and negative predictive value (high-sensitivity reading profile). Despite some overlap in the 95% CIs, the sum of the PI-RADS scores and the dominant parameter generally exhibited better accuracy among the study variables, and those two approaches should be further evaluated as alternative methods to represent the whole set of variables in the ESUR/PI-RADS scoring system.

Disclosures of Conflicts of Interest: L.K.B. disclosed no relevant relationships. G.L. disclosed no relevant relationships. C.A.H.v.d.K. Activities related to the present article: disclosed no relevant relationships. Activities not related to the present article: payment for lectures from ARRS. Other relationships: disclosed no relevant relationships. B.T. disclosed no relevant relationships. E.L.G. disclosed no relevant relationships. J.O.B. disclosed no relevant relationships.

References

- Sciarra A, Barentsz J, Bjartell A, et al. Advances in magnetic resonance imaging: how they are changing the management of prostate cancer. *Eur Urol* 2011;59(6):962–977.
- Eberhardt SC, Carter S, Casalino DD, et al. ACR Appropriateness Criteria prostate cancer—pretreatment detection, staging, and surveillance. *J Am Coll Radiol* 2013;10(2):83–92.
- Shao YH, Demissie K, Shih W, et al. Contemporary risk profile of prostate cancer in the United States. *J Natl Cancer Inst* 2009;101(18):1280–1283.
- Boccon-Gibod L, Bertaccini A, Bono AV, et al. Management of locally advanced prostate cancer: a European consensus. *Int J Clin Pract* 2003;57(3):187–194.
- Yamada AH, Lieskovsky G, Petrovich Z, Chen SC, Groshen S, Skinner DG. Results of radical prostatectomy and adjuvant therapy in the management of locally advanced, clinical stage TC, prostate cancer. *Am J Clin Oncol* 1994;17(4):277–285.
- Loeb S, Smith ND, Roehl KA, Catalona WJ. Intermediate-term potency, continence, and survival outcomes of radical prostatectomy for clinically high-risk or locally advanced prostate cancer. *Urology* 2007;69(6):1170–1175.
- Bostwick DG. Staging prostate cancer—1997: current methods and limitations. *Eur Urol* 1997;32(Suppl 3):2–14.

8. Hricak H, Choyke PL, Eberhardt SC, Leibel SA, Scardino PT. Imaging prostate cancer: a multidisciplinary perspective. *Radiology* 2007;243(1):28–53.
9. Fütterer JJ, Heijmink SW, Scheenen TW, et al. Prostate cancer: local staging at 3-T endorectal MR imaging—early experience. *Radiology* 2006;238(1):184–191.
10. Hegde JV, Chen MH, Mulkern RV, Fennessy FM, D'Amico AV, Tempny CM. Preoperative 3-Tesla multiparametric endorectal magnetic resonance imaging findings and the odds of upgrading and upstaging at radical prostatectomy in men with clinically localized prostate cancer. *Int J Radiat Oncol Biol Phys* 2013;85(2):e101–e107.
11. Brajtbord JS, Lavery HJ, Nabizada-Pace F, Senaratne P, Samadi DB. Endorectal magnetic resonance imaging has limited clinical ability to preoperatively predict pT3 prostate cancer. *BJU Int* 2011;107(9):1419–1424.
12. Barentsz JO, Richenberg J, Clements R, et al. ESUR prostate MR guidelines 2012. *Eur Radiol* 2012;22(4):746–757.
13. Portalez D, Rollin G, Leandri P, et al. Prospective comparison of T2w-MRI and dynamic-contrast-enhanced MRI, 3D-MR spectroscopic imaging or diffusion-weighted MRI in repeat TRUS-guided biopsies. *Eur Radiol* 2010;20(12):2781–2790.
14. Rosenkrantz AB, Kim S, Lim RP, et al. Prostate cancer localization using multiparametric MR imaging: comparison of Prostate Imaging Reporting and Data System (PI-RADS) and Likert scales. *Radiology* 2013;269(2):482–492.
15. Schimmöller L, Quentin M, Arsov C, et al. Inter-reader agreement of the ESUR score for prostate MRI using in-bore MRI-guided biopsies as the reference standard. *Eur Radiol* 2013;23(11):3185–3190.
16. Roethke MC, Kuru TH, Schultze S, et al. Evaluation of the ESUR PI-RADS scoring system for multiparametric MRI of the prostate with targeted MR/TRUS fusion-guided biopsy at 3.0 Tesla. *Eur Radiol* 2014;24(2):344–352.
17. Vos PC, Hambroek T, Barentsz JO, Huisman HJ. Computer-assisted analysis of peripheral zone prostate lesions using T2-weighted and dynamic contrast enhanced T1-weighted MRI. *Phys Med Biol* 2010;55(6):1719–1734.
18. Dickinson L, Ahmed HU, Allen C, et al. Magnetic resonance imaging for the detection, localisation, and characterisation of prostate cancer: recommendations from a European consensus meeting. *Eur Urol* 2011;59(4):477–494.
19. Hambroek T, Somford DM, Huisman HJ, et al. Relationship between apparent diffusion coefficients at 3.0-T MR imaging and Gleason grade in peripheral zone prostate cancer. *Radiology* 2011;259(2):453–461.
20. Hoeks CM, Hambroek T, Yakar D, et al. Transition zone prostate cancer: detection and localization with 3-T multiparametric MR imaging. *Radiology* 2013;266(1):207–217.
21. Fütterer JJ, Engelbrecht MR, Huisman HJ, et al. Staging prostate cancer with dynamic contrast-enhanced endorectal MR imaging prior to radical prostatectomy: experienced versus less experienced readers. *Radiology* 2005;237(2):541–549.
22. Epstein JI, Allsbrook WC Jr, Amin MB, Egevad LL; ISUP Grading Committee. The 2005 International Society of Urological Pathology (ISUP) consensus conference on Gleason grading of prostatic carcinoma. *Am J Surg Pathol* 2005;29(9):1228–1242.
23. van Veggel BA, van Oort IM, Witjes JA, Kiemeny LA, Hulsbergen-van de Kaa CA. Quantification of extraprostatic extension in prostate cancer: different parameters correlated to biochemical recurrence after radical prostatectomy. *Histopathology* 2011;59(4):692–702.
24. Jager GJ, Severens JL, Thornbury JR, de La Rosette JJ, Ruijs SH, Barentsz JO. Prostate cancer staging: should MR imaging be used?—A decision analytic approach. *Radiology* 2000;215(2):445–451.